

DARIUSZ MIKIELEWICZ* and TOMASZ MUSZYŃSKI

Experimental and theoretical study of surface cooling using a single microjet

Gdansk University of Technology, Faculty of Mechanical Engineering, Heat Technology Department, Narutowicza 11/12, 80-233 Gdańsk, Poland

Abstract

The experimental research of heat transfer due to impingement of a single microjet of water and air has been studied on a specially designed rig. Systematic data on radial wall temperature distribution were collected, which enabled development of empirical correlation for heat transfer coefficient applicable both for air and water flows. Two microjet nozzle diameters were studied, i.e. 180 and 260 μm . The correlation describing the heat transfer coefficient was later used in validation of a model of a single microjet impinging on a flat plate, developed earlier by the authors. Such analytical model of microjet is of a great value in future analysis as it enables to carry out for example sensitivity tests or to appropriately select operational parameters. The presented model is quite general and its further modifications are possible when some of the imposed assumptions are relaxed. More experiments on the structure of a single microjet are needed which will confirm the correlation presented in the paper.

Keywords: Surface cooling; Microjets; Heat transfer intensification

Nomenclature

- c_p – specific heat at constant pressure, J/kgK
- d – nozzle inner diameter, m
- G – mass velocity, kg/m²s
- \dot{m} – mass flow rate, kg/s

*Corresponding author. E-mail address: dmikiele@pg.gda.pl

Pr	–	Prandtl number
r	–	radial coordinate
q	–	heat flux density, W/m ²
q_v	–	volumetric generation of heat, W/m ³
\dot{Q}	–	rate of heat, W
t	–	wall thickness, m
T	–	temperature, K
g	–	gravity, m/s ²

Greek symbols

α	–	heat transfer coefficient, W/m ² K
λ	–	thermal conductivity, W/mK

Subscripts

A	–	radial direction in plate
c	–	convective
f	–	fluid
i	–	interface
s	–	plate bottom surface
w	–	wall

1 Introduction

Microjets have a number of industrial and medical applications which include microelectronics cooling (Kercher et al. [1], Wang et al. [2]), inkjet printing ([Hayes et al. [3]), precision manufacturing (Sibailly et al. [4]), drug delivery (Fletcher et al. [5]) and recently the microsurgery (Blumenkranz et al. [6], Fletcher et al. [7]). To date few highly local measurements have been made on microjets, due in part to the lack of techniques to investigate their characteristics and performance. Most reported studies have dealt with confined or submerged individual jets/jet arrays with conventional temperature measurement tools such as thermocouples (Mohanty et al. [8]) or thermochromic liquid crystals (Lee and Lee [9]). Little work has been published that investigates characteristics of individual, microscale free jets.

Tuckerman and Pease [10] demonstrated heat removal of 7.9 MW/m² with the flow rate of water equal to 516 ml/min using single-phase liquid convection in microchannels, and this work led to extensive research focusing on microchannel heat sinks with single-phase and two-phase cooling. Bowers et al. [11] showed that two-phase microchannels can remove over 2 MW/m² with flow rates of less than 65 ml/min and pressure drops of less than 30 kPa. Other microchannel studies include two-phase heat transfer modeling using the homogeneous flow assumption (Liu et al. [12]), or research into understanding of nucleation mechanisms and phase change phenomena (Zhang et al. [13]). Micromachined heat sinks incorporating liquid jets have recently received attention because they offer several

advantages over microchannels and other cooling methods. These advantages include the fact that the thin liquid boundary layer just outside of the impingement region promises higher heat removal rates. There are also problems associated with the use of impinging jet cooling systems such as stability of the jet for variable flow rates and fluid recovery. It ought to be remembered, however, that the technology of machining the microjets requires also the expertise on microchannels and their integral characteristics, as the pressure drop in such devices is of high importance. Very good surveys of possible capabilities and areas of application of microjets is given by Webb [14], Bar-Cohen et al. [15] and Agostini et al. [16].

There has been much experimental work on free liquid jet convection with jets featuring orifice diameters larger than 1mm (Jiang et al. [17], Stevens and Webb [18] and Womac et al. [19]). The models of convective heat transfer of impinging jets rely so far on the empirical correlations developed for conventional nozzle diameters, i.e. exceeding 1 mm. Their application to microjets may lead to amplification of errors, as can for example be seen in case of using correlations developed for flow boiling in conventional channels (diameters greater than 3 mm) to cases of flow boiling in microchannels. The stagnation Nusselt numbers were found to be constant for ratios of radial distance to orifice diameter less than 0.75 and relatively unaffected by nozzle to plate spacing. Garimella et al. [20] reported experimentally determined heat transfer coefficients as high as 60 kW/m²K. Boiling jet impingement can achieve significantly higher heat removal rates by utilizing the latent heat of vaporization. Jet impingement boiling characteristics which include subcooling, surface condition and velocity effects were experimentally examined for jets with orifice diameters greater than 1 mm (Li and Garimella [21], Ma and Bergles [22], Vader et al. [23], Wolf et al. [24]). These studies show that convective coefficients were relatively insensitive during fully developed boiling, where convection is dominated by the mixing induced by bubbles leaving the surface. However, fluid temperature and velocity have a significant impact on partial nucleate boiling, where the bubble population is typically low. In fully developed boiling, Wolf et al. [24] reported a heat flux removal of over 4 MW/m² with a wall superheat of 30–40 K and flow rate of water equal to 1.2×10⁵ ml/min.

Authors of the present paper have also been involved in studies of heat transfer in films formed due to impingement of single or two-phase jets on horizontal and inclined surfaces for different flow rates, nozzle diameters as well as thermal conditions. The studies were carried out both in laminar and turbulent flow regimes taking into account inertia, surface tension and shearing forces. All previous works have been collected in a monograph, D. Mikielewicz and J. Mikielewicz [25]. In these works considered also has been the distortion of velocity field as a result of nucleate boiling in the film. It ought to be stressed, however, that these stud-

ies were related to greater diameters of nozzles, i.e. $d > 1$ mm. In such case laminar and turbulent flow cases could be detected in heat transfer in films developing on the plate, whereas in case of microjets laminar cases are envisaged. In case of microjets, which are considered in the present paper, the assumed diameters of nozzles fall to much smaller values, not exceeding $260 \mu\text{m}$, however the results of the studies carried out earlier for laminar and turbulent film flows will be applicable in evaluation of heat transfer coefficient in films developed by impinging microjets.

In the paper an experimental study into a single microjet of water and air impinging on a solid surface will be presented. The profiles were studied of radial distribution of wall temperature. On that basis the correlation for heat transfer coefficient was elaborated. The experimental results were incorporated into the theoretical model of a single microjet [26]. The postulated in the paper approach has an advantage that the distribution of plate surface temperature will be a function of the nozzle supply parameters, namely flow rate of cooling liquid. The solutions to the model are in analytical form which increases the generality of the postulated model. In case of high heat fluxes, temperature of the plate may exceed the saturation temperature, which can cause nucleation of bubbles. That will even form a more efficient heat transfer mechanism. Such case was not studied in the present paper.

2 Experimental facility

A schematic of the water jet impingement test facility is presented in Fig. 1. The facility is versatile as it allows to test liquid and gas jets. The length of the nozzle used in experiments is 3 mm. Such length of the nozzle prevents excessive pressure losses and allows to create a laminar steady jet. Two different nozzle diameters, namely the inner diameters of $180 \mu\text{m}$ and $280 \mu\text{m}$ have been tested and will be discussed in the present study. The pressure of tap water, used in experiments, was controlled by air in the buffer tank. Induced pressure oscillations were eliminated in a pressure suppressor, which also served as water reservoir. Constant flow rate of water was obtained by sustaining the constant pressure of water with a proper use of flow control valve. Volumetric flow rate of water was measured at inlet and outlet from the cooling chamber with a graduated flask, as it is different at inlet and outlet due to evaporation of water as a result of contact with the hot surface, which causes that not the entire volume of water reaches the impingement surface and takes place in the cooling process. In experiment, four different supplying water gauge pressures were examined, namely 0.2, 0.4, 0.6 and 0.8 MPa, corresponding to volumetric flow rates of water of $G = 1\text{--}5$ ml/s. In case

of air cooling the gas is supplied directly from the pressure tank and was set to pressures of 0.2, 0.4, 0.6 and 0.8 MPa, respectively.

The cooled surface is the top surface of the cooper rod with 16 mm diameter. The radial distribution of surface temperature was measured using three T-type thermocouples, distributed along the radius, created by embedding a $50\ \mu\text{m}$ thick constantan wire to the rod's surface. Additional eight K-type thermocouples were attached at various locations in the cooper rod and the insulation. These thermocouples measure temperature gradient at the insulation surface of a heating block, in order to define heat losses to surroundings. They were connected to a second thermometer with a measuring range from $0\ ^\circ\text{C}$ to $1370\ ^\circ\text{C}$ and 1 K precision. The loss of applied power through conduction into the insulation and radiation to the surroundings was accurately calculated and accounted for in all tests. Data were collected from steady state measurements in order to exclude heat capacity of the installation. Another coated thermocouple was measuring the water film temperature on impingement surface. The thermocouples were connected to thermometer with the measuring range from $-50\ ^\circ\text{C}$ to $+200\ ^\circ\text{C}$ and 0.1 K precision. Heat was supplied to the rod by a ceramic heater wound around the rod. The whole arrangement was insulated and placed in the casing. The ceramic heater was powered by a 0-230 VAC variac (autotransformer) and total power input was measured by a LW-1 type wattmeter, Fig. 1.

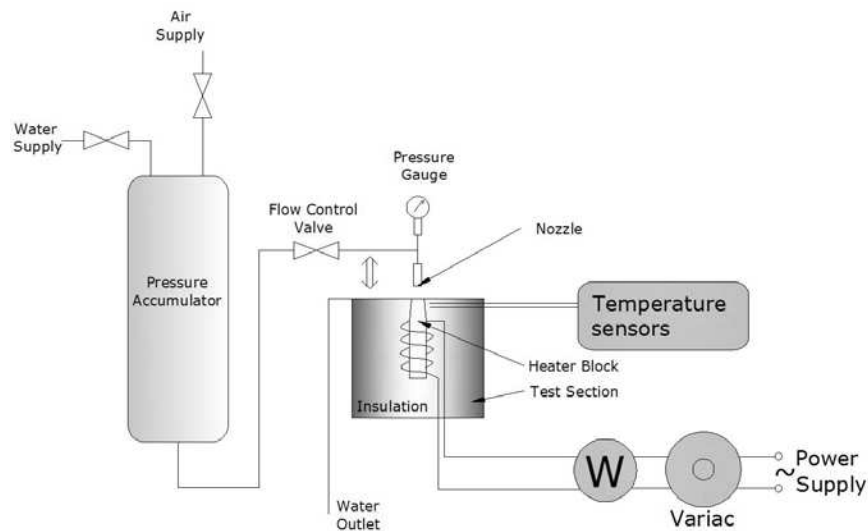


Figure 1. General schematic of test facility.

Values of the heater operating power were controlled and measured. As mentioned earlier, the heating element, Fig. 2, was a copper rod on which a resistance wire coated with ceramics was wound up.

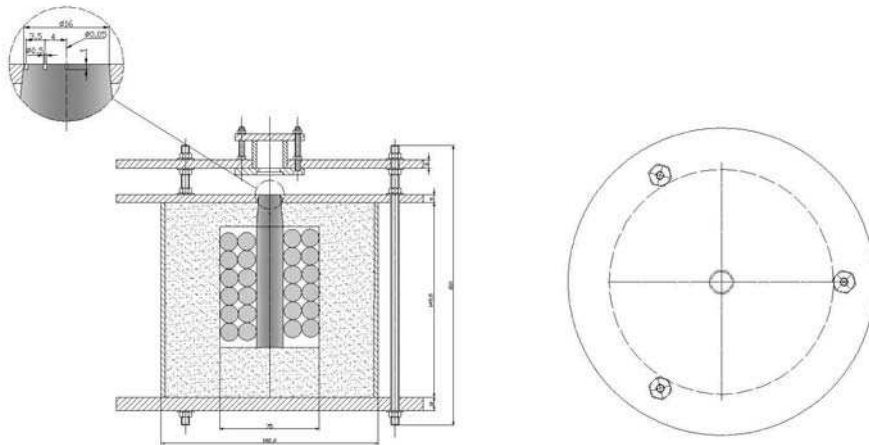


Figure 2. Schematic of heating section.

In order to perform measurements of the plate surface the T type thermocouples with diameter of $50 \mu\text{m}$ have been used, Fig. 3. On the radius of the plate four such thermocouples were embedded from below in a specially cut groove. Thermocouples were radially distributed 2 mm apart from each other.

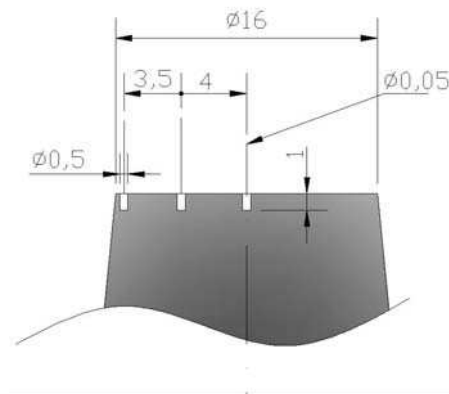


Figure 3. Distribution of thermocouples on the copper rod surface.

3 Theoretical model

When a liquid jet impinges on a surface, a very thin layer of liquid film is formed. Consequently, very high heat transfer coefficients can be obtained. Basic dimensions in the spreading film, assumed in the present study, together with flow

configuration are shown in Fig. 4. A 1-D radial model has been developed, which accounts for conduction of heat in the solid and convection within the liquid film. The model, as shown in Fig. 4, assumes that the liquid boundary layer develops from the jet impingement in the surroundings of air.

The problem is considered with the following assumptions:

1. Heat transfer coefficient, α , plate thermal conductivity, λ_w , mass flow rate of liquid, \dot{m} , volumetric heat generation, q_v , are constant.
2. There is no transfer of heat to surroundings and only to the cooling film (the bottom of the considered plate as well as the boundaries of the plate were perfectly insulated).

In Fig. 5 presented is the schematic for energy balance in arbitrary control volume for the film flow and in Fig. 6 the corresponding one in the plate with internal heat generation.

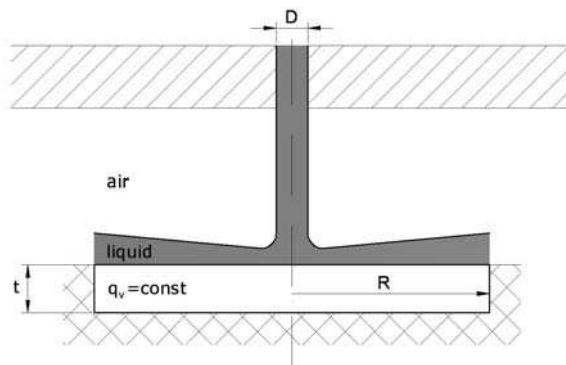


Figure 4. Schematic of impinging jet.

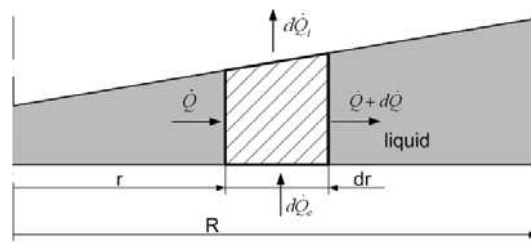


Figure 5. Schematic for energy flow in the fluid.

In case of the film, the energy balance on the control volume considers the change of mean film temperature due to convective heating of the film, $d\dot{Q}_c$, and the interface heat transfer, $d\dot{Q}_i$. The value of the term $d\dot{Q}_i$ in the present study

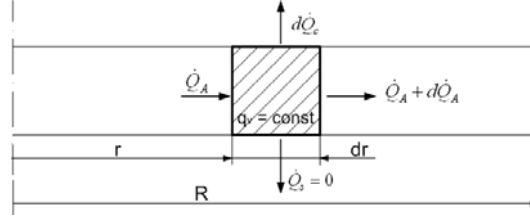


Figure 6. Schematic for energy flow in the plate.

has been set to zero, as it has been assumed that the whole heat is accumulated in the liquid film, however, the obtained solution permits for the analysis of that influence. Therefore the governing energy equation for the fluid yields:

$$\dot{m}c \frac{dT_f}{dr} = 2\pi r \alpha (T_w - T_f). \quad (1)$$

In line with the assumptions, the base of the plate is perfectly insulated ($\dot{Q}_S = 0$) and the energy balance to the plate therefore yields:

$$\lambda_w \frac{d}{dr} \left(r \frac{dT_w}{dr} \right) + q_v r = \frac{r \alpha}{t} (T_w - T_f). \quad (2)$$

In Eqs. (1) and (2) T_w and T_f represent mean local temperatures of the wall and the fluid respectively. Solution to Eqs. (1) and (2) results in the distribution of temperature of wall and cooling fluid. In order to obtain such solution we need information on the heat transfer coefficient in the flow of film. Iterative solution of (1) and (2) enables analytical determination of fluid and wall temperature distributions for the considered fluid and plate.

Temperature of cooling fluid distribution yields:

$$\dot{m}c \frac{dT_f}{dr} + 2\pi r \alpha T_f = 2\pi r \alpha \left[q_v t \left(\frac{1}{\alpha} + \frac{\pi}{\dot{m}c} r^2 \right) + T_{f0} \right]. \quad (3)$$

Equation (3) can be solved as a non-homogeneous differential equation with constant coefficients. The result will consist of a solution to homogeneous equation and subsequently parametrisation of the constant will be carried out. The homogeneous equation reads:

$$\frac{dT_f}{T_f} = -\frac{2\pi r \alpha}{\dot{m}c} dr. \quad (4)$$

The solution to Eq. (4) yields:

$$T_f = C_2(r) \exp \left(-\frac{\pi \alpha r^2}{\dot{m}c} \right). \quad (5)$$

The specific solution to (3) is obtained through parametrisation of the constant present in (5):

$$C_2(r) = \left[T_{f0} + \frac{\pi q_v t}{\dot{m}c} r^2 \right] \exp\left(-\frac{\pi \alpha r^2}{\dot{m}c}\right) + C_3. \quad (6)$$

The constant $C_3 = 0$ results from the boundary condition:

$$\text{for } r = 0 \quad T = T_{f0}. \quad (7)$$

Distribution of fluid temperature enables to determine the distribution of wall temperature:

$$T_w = T_{w0} + \frac{1}{16} \frac{\pi q_v \alpha}{\dot{m} c_p \lambda_w} r^4. \quad (8)$$

In (8), the wall temperature at the stagnation point T_{w0} is used, which represents the initial wall temperature in experiments at the stagnation point.

4 Results of calculations

In the course of performed experiments the radial distributions of plate temperatures have been recorded for the case of two nozzle dimensions, namely 160 μm and 260 μm . Two fluids were examined, namely air and water. Equations (3) and (8) require appropriate values of heat transfer coefficient in order to accomplish calculations with the objective to obtain wall temperature distribution. For that reason an empirical correlation has been elaborated. The experimentally collected heat transfer coefficient was approximated using the multiple regression method to yield the following relation:

$$\alpha = 77 \dot{m}^{0.88} d^{-0.11} \text{Pr}^{-2}. \quad (9)$$

The developed correlation has a simple form, dependent only of mass flow rate \dot{m} (expressed in ml/s) and diameter of the nozzle (expressed in mm). The Prandtl number is for the sake capturing the specific properties of different fluids, here water and air. Comparisons against authors own experimental data are presented in Fig. 7 for the case of water and Fig. 8 for air, respectively. Experimental values of heat transfer coefficient were determined directly from the Newton's law, i.e. as a ratio of applied heat flux to the temperature difference between local wall temperature and temperature of fluid in the nozzle:

$$\alpha = \frac{q}{(T_w(r) - T_{f0})}. \quad (10)$$

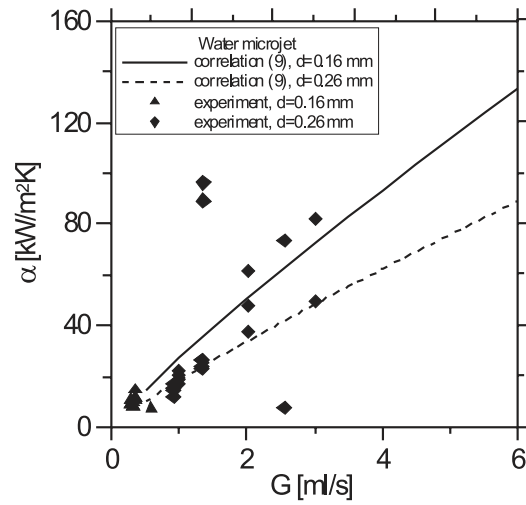


Figure 7. Fit to experimental data for two nozzle diameters, 180 and 260 μm to data for water.

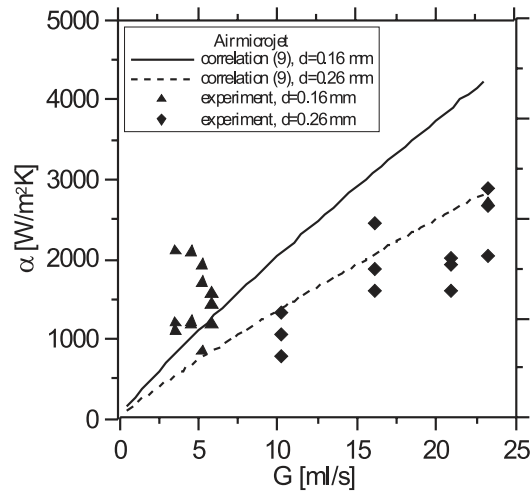


Figure 8. Fit to experimental data for two nozzle diameters, 180 and 260 μm to data for air.

Values of heat transfer coefficient are crucial in calculations of wall temperature distribution. Sample distributions of wall temperature are presented in Fig. 9 to 11, whereas those for air are in Fig. 12 to 14. In these figures shown also are the calculations of wall temperature obtained by means of Eq. (8), presented in the previous section.

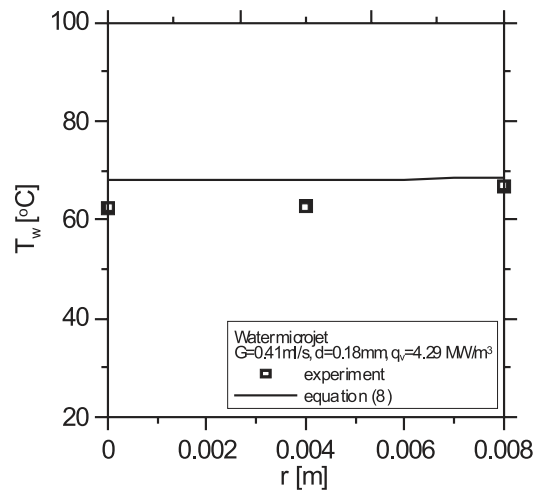


Figure 9. Wall temperature distribution on a plate after water microjet impingement, $d = 80 \mu\text{m}$, $\dot{m} = 0.41 \text{ ml/s}$.

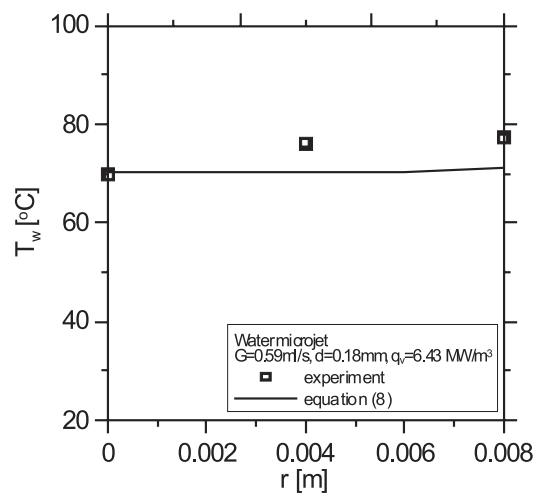


Figure 10. Wall temperature distribution on a plate after water microjet impingement, $d = 180 \mu\text{m}$, $\dot{m} = 0.59 \text{ ml/s}$.

We can observe that the consistency of both wall temperature distributions is satisfactory, however the agreement between the model calculations and experimental data is much better in case of water than air. That is probably due to the fact measurements of the bulk temperature in case of air jet impingement is much more prone to errors.

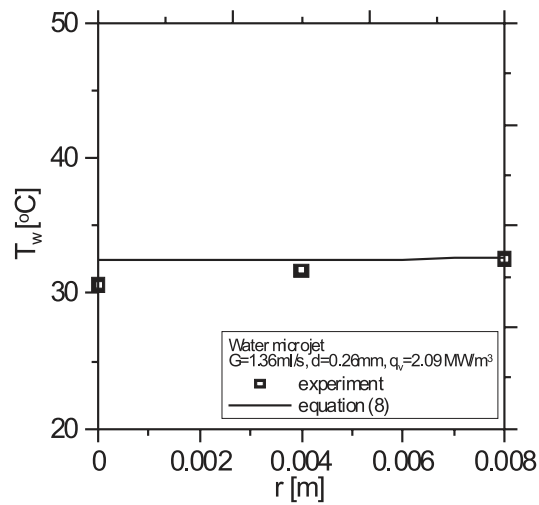


Figure 11. Wall temperature distribution on a plate after water microjet impingement, $d = 260\ \mu\text{m}$, $\dot{m} = 1.36\ \text{ml/s}$.

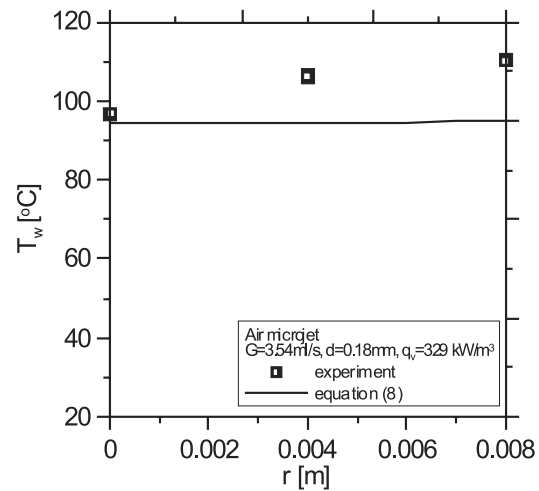


Figure 12. Wall temperature distribution on a plate after air microjet impingement, $d = 180\ \mu\text{m}$, $\dot{m} = 3.54\ \text{ml/s}$.

5 Conclusions

The experimental research of heat transfer due to impingement of a single microjet of water and air was studied on a specially designed rig. Systematic data on radial wall temperature distribution have been collected, which enabled development of empirical correlation for heat transfer coefficient. Two microjet nozzle

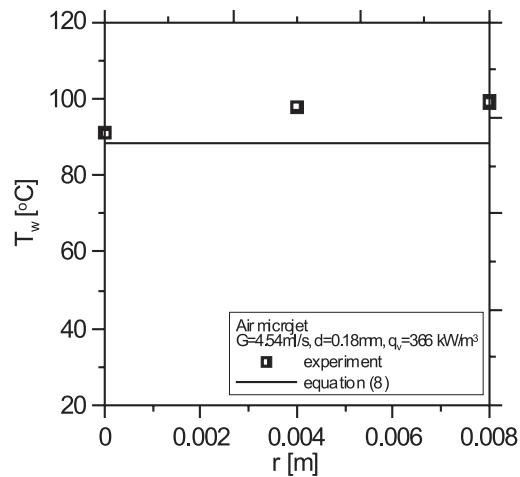


Figure 13. Wall temperature distribution on a plate after air microjet impingement, $d = 180 \mu\text{m}$, $\dot{m} = 4.54 \text{ ml/s}$.

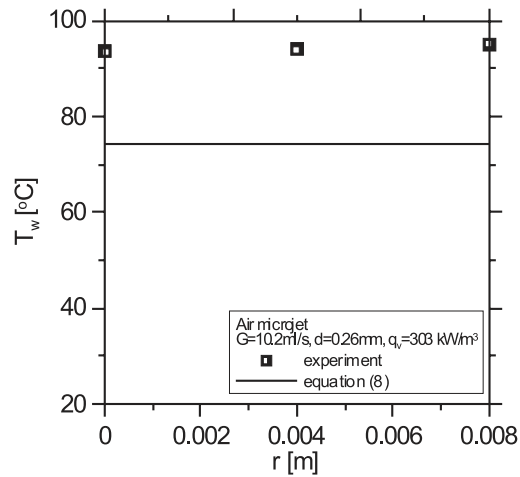


Figure 14. Wall temperature distribution on a plate after air microjet impingement, $d = 260 \mu\text{m}$, $\dot{m} = 10.2 \text{ ml/s}$.

diameters were studied, i.e. 180 and $280 \mu\text{m}$. That correlation was later used in validation of a model of a single microjet developed earlier by the authors [26].

Presented also has been a solution to a conjugate problem of temperature distribution in the liquid film as well as in the wall. Qualitatively, the model returns good results which allows the discussion of the influence of various parameters on temperature field and optimize the thermal load of microprocessor. Such tool would be very helpful in planning of experiments with other cooling fluids.

A simple form of distribution of wall temperature and cooling fluid temperature obtained in analytical model is of a great value when the sensitivity tests are to be carried out. That will enable, for example the optimization of parameters consisting for the method of cooling. The model is quite general and its further modifications are possible when some of the assumptions are relaxed. The performance of presented model depends very strongly on the distribution of heat transfer coefficient. More experiments on the structure of a single microjet are needed which will confirm the heat transfer coefficient correlation presented in the paper.

Acknowledgements Authors would like to appreciate the funding from the Ministry for Science and Higher Education research grant R 06 011 03 in years 2007–2010.

Received 30 January 2010

References

- [1] Kercher D.S., Lee J., Brand O., Allen M.G., Glezer A.: *Microjet cooling devices for thermal management of electronics*. IEEE Trans. Comp. Pack. Technol. **26**(2003), 359–366.
- [2] Wang E.N., Zhang L., Jiang L., Koo J.-M., Maveety J.G., Sanchez E.A., Goodson K.E., Kenny T.W.: *Micromachined jets for liquid impingement cooling of VLSI chips*. J. Microelectromech. Syst. **13**(2004), 833–842.
- [3] Hayes D.J., Wallace D.B., Cox W.R.: *Microjet printing of solder and polymers for multi-chip modules and chip-scale packages*. Proc. SPIE Int. Conf. High Density Pack. MCMs. 3830, 1999, 242–247.
- [4] Sibailly O.D., Wagner F.R., Mayor L., Richerzhagen B.: *High precision laser processing of sensitive materials by microjet*. Proceedings of the Fourth International Symposium on Laser Precision Microfabrication, 2003, 501–504.
- [5] Fletcher D.A., Palanker D.V.: *Pulsed liquid microjet for microsurgery*. Appl. Phys. Lett. **78**(2001), 1933–1935.
- [6] Blumenkranz M.S., Palanker D.V., Fletcher D., Miller J.: *A pulsed liquid microjet for ocular microsurgical applications*. Inv. Ophthalmol. Vis. Sci. **42**(2001), S717–S1717.
- [7] Fletcher D.A., Palanker D.V., Huie P., Miller J., Marmor M.F., Blumenkranz M.S.: *Intravascular drug delivery with a pulsed liquid microjet*. Arch. Ophthalmol. **120**(2002), 1206–1208.

-
- [8] Mohanty A.K., Tawfek A.A.: *Heat-transfer due to a round jet impinging normal to a flat surface*. Int. J. Heat Mass Transfer **36**(1993), 1639–1647.
- [9] Lee J., Lee S.J.: *Stagnation region heat transfer of a turbulent axisymmetric jet impingement*. Exp. Heat Transfer **12**(1999), 137–156.
- [10] Tuckerman D.B., Pease R.F.W.: *High-performance heat sinking for VLSI*. IEEE Electron Device Lett. **EDL-2**(1981), 126–129.
- [11] Bowers M., Mudawar I.: *High-heat flux boiling in low-flow rate, low-pressure drop mini-channel and microchannel heat sinks*. Int. J. Heat Mass Transfer **37**(1994), 321–332.
- [12] Liu X., Lienhard V.J.H., Lombara J.S.: *Convective heat transfer by impingement of circular liquid jets*. J. Heat Transfer **113**(1991), 571–582.
- [13] Zhang L., Koo J.-M., Jiang L., Asheghi M., Goodson K.E., Santiago J.G., Kenny T.W.: *Measurements and modeling of two-phase flow in microchannels with nearly-constant heat flux boundary conditions*. J. Microelectromech. Syst. **11**(2002), 12–19.
- [14] Webb R.L.: *Next generation devices for electronic cooling with heat rejection to air*. Trans. ASME **127**(2005), 2–10.
- [15] Bar-Cohen A., Arik M., Ohadi M.: *Direct liquid cooling of high heat flux micro and nano electronic equipment*. Proc. of the IEEE **94**(2006), 1549–1570.
- [16] Agostini B., Fabbri M., Park J.E., Wojtan L., Thome J.R., Michael B.: *State of the art of high heat flux cooling technologies*. Heat Transfer Engineering **28**(2006), 258–281.
- [17] Jiang L., Wong M., Zohar Y.: *Phase change in microchannel heat sinks with integrated temperature sensors*. J. Microelectro-mechanical Systems **8**(1999), 358–365.
- [18] Stevens J., Webb B.W.: *Local heat transfer coefficients under an axisymmetric, single-phase liquid jet*. J. Heat Transfer **113**(1999), 71–78.
- [19] Womac D.J., Ramadhyani S., Incropera F. P.: *Correlating equations for impingement cooling of small heat-sources with single circular liquid jets*. J. Heat Transfer **115**(1993), 106–115.
- [20] Garimella S.V., Rice R.A.: *Confined and submerged liquid jet impingement heat-transfer*. J. Heat Transfer **117**(1995), 871–877.
- [21] Li C.Y., Garimella S.V.: *Prandtl-number effects and generalized correlations for confined and submerged jet impingement*. Int. J. Heat Mass Transfer **44**(2001), 3471–3480.
- [22] Ma C.F., Bergles A.E.: *Jet impingement nucleate boiling*. Int. J. Heat Mass Transfer **29**(1985), 1095–1101.

- [23] Vader D.T., Incropera F.P., Viskanta R.: *Convective nucleate boiling on a heated surface cooled by an impinging planar jet of water*. J. Heat Transfer **114**(1992), 152–160.
- [24] Wolf D.H., Incropera F.P., and Viskanta R.: *Local jet impingement boiling heat transfer*. Int. J. Heat Mass Transfer **39**(1996), 1395–1406.
- [25] Mikielwicz D., Mikielwicz J.: *Surface cooling by means of axially symmetrical liquid jets*. Gdansk University of Technology Publishers, Gdansk 2005.
- [26] Mikielwicz D., Mikielwicz J.: *Analytical model of single microjet cooling of electronic equipment*. Proc. of the Sixth Int. ASME Conf. on Nanochannels, Microchannels and Minichannels, ICNMM2008, June 23-25, 2008, Darmstadt, Germany, paper ICNMM2008-62173.